International Journal For Advanced Research In Science & Technology
A peer reviewed international journal
www.ijarst.in
ISSN: 2457-0362

SINGLE-LEGGED JUMPING ACTION SIMULATION WITHOUT DISRUPTING THE STRUCTURE

POLAMURI RAMA MOHAN REDDY 1, PRAVEEN KUMAR MUNNANGI 2,
ASSOCIATE PROFESSOR 1, ASSISTANT PROFESSOR 2,
Mail ID:polamurirammohanreddy@gmail.com, Mail ID:praveenmunnangi009@gmail.com
Dept.: Mechanical
Pallavi Engineering College,
Kuntloor(V),Hayathnagar(M),Hyderabad,R.R.Dist.-501505.

abstract

There are many different kinds of mechanical and biomechanical systems in people's environments, and they may come into touch with them in many different ways. Here, we use a structure-preserving approach to the simulation of the dynamics of a monopodial jumper, who is modelled as a three-dimensional stiff multibody system with contact. The idea of Lagrange d'Alembert, upon which the applied mechanical integrator is founded, is modified to account for practical constraints. This new variational integrator for multibody dynamics maintains the smecticity and momentum maps. Instead of relying on a smooth approximation of the contact issue through a penalty potential, we address the non-smooth problem, which includes the calculation of the contact configuration, time, and force, to guarantee the structure's preservation and geometric correctness. For this reason, we are also curious in the optimum control of the one-legged high leap, in addition to the formulation of non-smooth issues in forward dynamic simulations. A direct transcribing approach (see [14]) is used to solve the optimum control issue by recasting it as a restricted optimization problem.

Introduction

The human locomotor system is the subject of a great deal of biomechanical literature, with many studies focusing on walking motions [5, 17]. Actions involving leaping, such as those seen in [1], are of particular importance here. In our simulation, the monopodial jumper is modelled as a multi-body system with constraints, and its forward dynamics and optimum control issue are simulated in a non-smooth fashion. Locomotion on two legs, as opposed to four wheels, necessitates simulation approaches to deal with the establishing and breaking of contact between the foot and the ground. The studied contact formulation encompasses the notion of perfectly elastic and perfectly plastic contacts (for example, see [8]), with the latter meaning that the foot maintains contact with the ground for a fixed period of time.

The monopodial jumper model's top half represents the torso, while the lower half is made up of two stiff bodies joined at the knee. When the knee is taken into account, the resulting movement is distinct from the technically oriented jumpers discussed, for example, in [7, 12]. By include both the perfectly elastic and ideally plastic contact formulations in the forward dynamic's simulations, the critical times at which contact is established and broken may be calculated. By minimizing a cost function with a physiologically driven objective, the ideally controlled jumper permits actuation at the hip and the knee. In the numerical solution, the optimum control issue is converted into an optimization problem subject to satisfying discrete equations of motion, boundary conditions, and route restrictions, as shown for example in [10, 18]. To prevent the optimization issue from being artificially constrained by dictating the time at which contact is established or severed, variable time steps are employed, with two scaling factors being part of the optimization parameters.

Configuration and motion of a rigid multibody system

For this study, we use the rotation-free formulation described in [2] for rigid bodies and in [4] for rigid multibody systems to describe the configuration of the simulated bodies and hence simulate their dynamics. The configuration vector q (t) R 12 for the twelfth rigid body is made up of the coordinates for its center of mass (t) and the coordinates for the right-handed director triad d I (t) for I = 1, 2, and 3. The director triad defines the body's spatial orientation and must remain orthogonal while in motion in the space under consideration.

period [t0, TN] ensured by six 'internal restrictions' gINT (q) = 0 R 6. Different kinds of joints, such as revolute or spherical joints, link the rigid bodies in multibody systems. A scleronomic and holonomic constraint function g(q) R m on the redundant configuration variable q R k, where k = 12 times the number of bodies, is generated by the interconnectedness and stiffness of the bodies. Directly acting on the multibody systems is the independent generalized force R km, and the resultant k-dimensional redundant actuation f(q) R k may be calculated using the input transformation matrix B T (q) R k(km) and the formula f(q) = B T (q). Notably, the transformation matrix is dependent on the intercomsection of the rigid bodies, and its specifics are detailed in [14].

Integration while conserving structure in limited mechanical systems

International Journal For Advanced Research In Science & Technology
A peer reviewed international journal www.ijarst.in
IJARST
ISSN: 2457-0362

The Lagrangian or Hamiltonian formalism may be used to explain the dynamics of continuous mechanical systems. An integrator that maintains the original structure is derived in this context using discrete Lagrangian mechanics (for reference, see [16]). The time-dependent configuration vector q(t) Q is used in a configuration main fold to analyse the limited mechanical system. According to the method described in [14], the restricted Lagrange d'Alembert principle may be discretized at the time nodes t=t0, t=t1 = t0 + t, t=Tn = t0 + nt, t=TN = t0 + Tn, where NN is the number of time intervals, and the resulting discrete configurations qn q(Tn) approx. The Lagrange multipliers may be approximated by (t) R m if n (Tn). The action integral of the continuous Lagrangian over a single time interval is approximated by the discrete Lagrangian Ld.: Q Q R, as is customary in the setting of discrete variational mechanics. Thus, the resultant action total must be stationary according to the discrete Lagrange-d'Alembert principle.

$$\delta S_d = \delta\left[\sum_{n=0}^{N-1} L_d(\boldsymbol{q}_n, \boldsymbol{q}_{n+1}) - \frac{1}{2}(t_{n+1} - t_n)\left[\boldsymbol{g}^T(\boldsymbol{q}_n)\cdot\boldsymbol{\lambda}_n - \boldsymbol{g}^T(\boldsymbol{q}_{n+1})\cdot\boldsymbol{\lambda}_{n+1}\right]\right] + \sum_{n=0}^{N-1} \boldsymbol{f}_n^- \cdot \delta\boldsymbol{q}_n + \boldsymbol{f}_n^+ \cdot \delta\boldsymbol{q}_{n+1} = \boldsymbol{0}$$

for all possible combinations of q and n. This results in the constrained forced discrete Euler-Lagrange equations in dimension (k + m).

$$D_2L_d(q_{n-1},\ q_n) + D_1L_d(q_n,\ q_{n+1}) - G_d^T(q_n)\cdot\lambda_n + f_{n-1}^+ + f_n^- = 0$$
$$g(q_{n+1}) = 0,$$

problems with optimum control

Finding the state trajectory and force field that will take a system from its initial state to a desired destination is the goal of optimum control issues. End state, or q(t0) = q0, q (t0) = q 0 Simply put, q(TN) = qN, and q (TN) = q N. The system under investigation satisfies both the equations of motion and the required functional.

$$J(\boldsymbol{q}, \dot{\boldsymbol{q}}, \boldsymbol{f}) = \int_{t_0}^{t_N} C(\boldsymbol{q}, \dot{\boldsymbol{q}}, \boldsymbol{f})\ dt$$

is minimized under the cost function C (q, q), where TQT qQR is a known cost function. The optimum control problem is handled by first transforming it into a restricted optimization problem using a direct transcription approach. Approximating the integral of the continuous cost function, the discrete objective function is used in discretely restricted optimization situations.

$$\min_{\boldsymbol{u}_d, \boldsymbol{\tau}_d} \overline{J}(\boldsymbol{u}_d, \boldsymbol{\tau}_d) = \min_{\boldsymbol{u}_d, \boldsymbol{\tau}_d} \sum_{n=0}^{N-1} \overline{C}(\boldsymbol{u}_n, \boldsymbol{u}_{n+1}, \boldsymbol{\tau}_n),$$

subject to the constraints given by the reduced discrete equations of motion of the simplistic momentum scheme in

$$P^T(q_n)\cdot\left[D_2L_d(q_{n-1}, q_n) + D_1L_d(q_n, F_d(u_{n+1}, q_n)) + f_{n-1}^+(q_n, \tau_{n-1}) + f_n^-(q_n, \tau_n)\right] = 0 \quad .$$

In addition to the discrete equations of motion of the specific mechanical integrator, further constraints, like initial conditions, final conditions and possible inequality path constraints can be imposed.

Leaper who only uses one foot

The monopodial jumper's three-dimensional design was motivated by the human locomotor apparatus. In order to better understand the factors that contribute to a successful leap, we use a simplified model consisting of three rigid bodies (representing the lower leg, upper leg, and trunk, respectively; see Figure 1). While the hip is represented by a spherical joint, the human knee is modelled as a revolute joint with the rotation axis specified by the unit vector n1 in body 2. The angle between the thigh and the calf is less than because, in actuality, the allowable angles of anatomical joints are limited; for example, in the optimal control issue, an inequal its constraint function h3d(q) 0 prohibits the human knee from super-extending. As the upper body is supported by a prismatically joint, it can only move in a direction perpendicular to e3, making rotation along this axis impossible. Internal limitations are present in the monopodial jumper's con strained system, characterized as a 36-dimensional configuration variable owing to the stiffness mint = 18. Since the model is limited by m = 31 holonomic constraints and the joint linkages create met = 13 external constraints, it is clear that m >= 13 is required. Cor

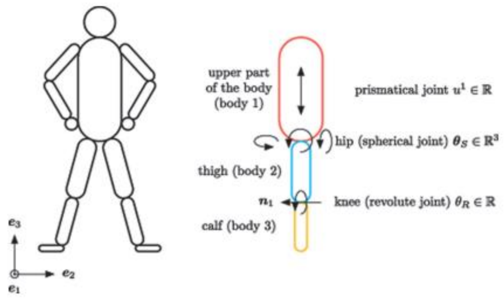

Figure 1: Three-dimensional jumper model with generalized coordinates and actuations that react to k + m = 5 degrees of freedom.

$$\boldsymbol{u} = \begin{bmatrix} u^1 \\ \boldsymbol{\theta}_S \\ \boldsymbol{\theta}_R \end{bmatrix} \in \mathbb{R}^5 \quad \text{and} \quad \boldsymbol{\tau} = \begin{bmatrix} \tau^1 \\ \boldsymbol{\tau}_S \\ \boldsymbol{\tau}_R \end{bmatrix} \in \mathbb{R}^5$$

with a force perpendicular to e3, and a translational velocity of u 1 R. The calf's relative rotation, denoted by the vector R R 3, and the hip's, denoted by the vector S R 3, are both rotary in nature (see Figure 1 for details). The torques S R 3 and R R work at the knee joint to move the hip of the monopodial jumper.

Communication-Based Methodology

The physics behind totally elastic and perfectly plastic connections is addressed inside the forward dynamic's simulation of the monopodial jumper. If the contact force is sufficient to keep the foot from penetrating the earth, then the jumper will not lose their footing. Since the model of a foot's ground contact during a leap predicts that the foot will lift as soon as the contact force is zero, the foot should be released as soon as the contact force changes sign.

Cohesive Contact Elasticity Formulation

For chains of point masses within a box, the modelling of fully elastic interactions using a variational integrator is carried out in [15], with further information available in [6]. Here, the distance between the foot and the ground, where the ground is the (e1, e2)-plane, is specified by the implemented non-penetration condition vc(q) 0 R. (see Figure 2). Using the discrete Euler-Lagrange equations in Equation (with a constant time step t), the forward dynamics simulation determines a new configuration qn+1 as long as the non-penetration criterion is not broken (1-2). Each time step concludes with a check for whether or not the inequality constraint holds for the latest configuration qn+1. In the event that it is broken, the configuration qn+1 is thrown out (for example, the dashed configuration in Figure 2), and the physically correct contact configuration q must be determined.

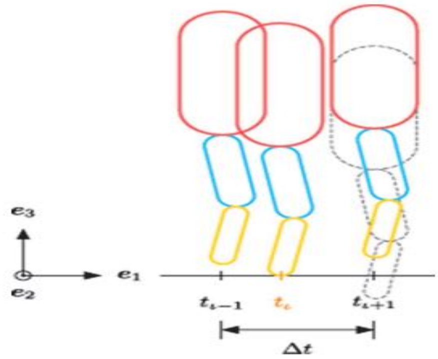

Fig. 2. Perfectly elastic contact

Physical quantities of the calf, thigh (taken from [19]) and the human torso (taken from [9] with a total weight of 64.90 [kg])

physical quantity	calf	thigh	torso
mass [kg]	3.2800	6.8600	28.2055
moment of inertia [kgm^2]			
$I_{e_1e_1}$	0.0490	0.1238	0.1368
$I_{e_2e_2}$	0.0504	0.1188	0.1368
$I_{e_3e_3}$	0.0037	0.0229	0.9035

Exhibit Numbers

In the completely elastic contact formulation, energy conservation is a crucial factor. Using a straight-leg example, we can see how the energy behaves with time. Table 1 displays various anthropometric data about the human body, including the chest, the legs, and the thighs. Starting from a stationary position, the calf's center of gravity is located at [0, 0, 0.5] m. This motion lasts for 400 s, during which time more than 830 interactions are recorded. The long-term energy behaviour of the algorithm is presented in Figure 3; it exhibits a minor fluctuation of the total energy (as is common for variational integrators), but the method does not squander energy numerically. In [11], the completely elastic contact formulation is explained in further depth, and another example is provided.

International Journal For Advanced Research In Science & Technology
A peer reviewed international journal www.ijarst.in
IJARST
ISSN: 2457-0362

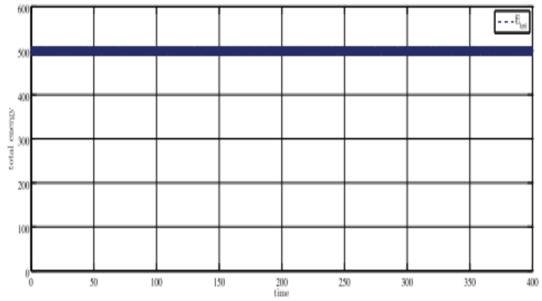

Fig. 3. Energy evolution for 830 contacts

Sustaining optimum command of the monopodial bounder

The optimum control problem seeks to determine the most efficient path from the start to the end states that the jumper may take. Here, the jumper is only activated at the hip and knee, unlike the aforementioned instances. For the initial state of the optimum control issue, the foot is in touch with the ground, which is modelled as a completely plastic contact. The optimum control issue involves a motion with a contact and a flying phase, as shown in Figure 10. By the conclusion of the flight phase, the maximum leap height must be achieved.

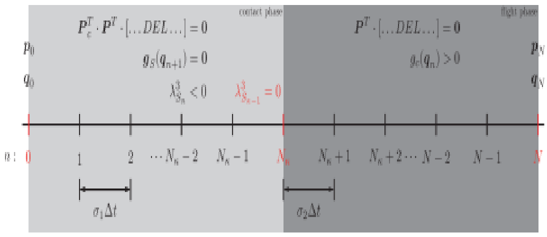

Fig.4 further reduction is achieved by applying the nodal reparameterization of the flight phase Fd from $q_{n+1}=F_d$ (u_{n+1},q_n)(fulfilling the constraints g(qn+1) = 0 in

$$D_2L_d(q_{n-1},q_n)+D_1L_d(q_n,q_{n+1})-G_d^T(q_n)\cdot\lambda_n-(G_S^T)_d(q_n)\cdot\lambda_{S_n}+f_{n-1}^+ + f_n^- = 0$$

)). Since this is the case, the contact phase's forced discrete equations of motion are likewise reduced to a 5-dimensional system. It's important to note at this juncture that the aforementioned monopodial jumper has two degrees of freedom during the collision phase. However, a new highly nonlinear nodal reparameterization is needed for the greatest possible decrease (involving trigonometric functions). The optimiser can function more quickly and easily with a somewhat greater number of dynamical constraints if they are less nonlinear, as has been shown in practice. For forward dynamics simulations, the contact force inhibits ground penetration, and when the contact force reverses sign, the algorithm determines when the contact may be released and what configuration it should take. Inequality path constraints provide the right direction of the contact force, i.e., the correct sign of the Lagrange multiplier 3 Sn 0 for n = 1, 2, during the contact phase of the optimum control problem. However, the contact force is not present since it is remultiplied out by the contact null space matrix Pc(qn).

$$P_c^T(q_n)\cdot P^T(q_n)\cdot\left[D_2L_d(q_{n-1},q_n)+D_1L_d(q_n,q_{n+1})+f_{n-1}^+ + f_n^-\right]=0$$

. As a result, the Lagrange multiplier associated with the contact phase optimum control issue has to be recalculated after each time step to ensure it has the right sign, indicating that it satisfies the inequality route requirements. Multipliers of the contact Lagrange may be determined via.

$$\lambda_{S_n} = S^T(q_n)\cdot P^T(q_n)\cdot\left[D_2L_d(q_{n-1},q_n)+D_1L_d(q_n,q_{n+1})+f_{n-1}^+ + f_n^-\right],$$

with $S(q_n)=P^T(q_n)\cdot G_S^T(q_n)\cdot\left(G_S(q_n)\cdot P(q_n)\cdot[G_S(q_n)\cdot P(q_n)]^T\right)^{-1}\in\mathbb{R}^{5\times3}.$

Guaranteed by the boundary constraints h1d (q0, p0) = 0 R 2, the initial state of the jumper is q(t0) = q 0, p(t0) = p 0 where p 0 R 36 is the initial conjugate momentum. To keep the jumper confined to the (e1, e3) plane, we employ a path restriction function h2d(qn) = 0 such that the only torques acting on the jumper are in the e2-direction. The release time and the height of a monopodial leap are both heavily influenced by the actuation of the jumper during the contact period. It is part of the optimal control issue to determine the optimum contact release time, which is not known in advance. The contact release time node tN is implemented with a known node number N, but the corresponding physical time TN is a variable that must be calculated via optimization. Therefore, the parameters 1, 2 R (see Figure 10) are scalars that are included in the optimization variables, and they scale the time steps before and after the contact release time. The one-legged hoppers' restricted optimisation challenge is solved.

$$\min_{u_d,\tau_d,\sigma_1,\sigma_2} \tilde{J}_d(u_d,\tau_d,\sigma_1,\sigma_2)$$

Subject to

reduced forced discrete equations of motions during the contact phase for $n=1,\dots,K$

$$P_c^T(q_n)\cdot P^T(q_n)\cdot\left[D_2L_d(q_{n-1},q_n)+D_1L_d(q_n,q_{n+1})+f_{n-1}^+ + f_n^-\right]=0$$

$$g_S(\boldsymbol{q}_{n+1}) = \boldsymbol{0}$$

reduced forced discrete equations of motions during the flight phase $n = \kappa + 1, \ldots, N-1$

$$\boldsymbol{P}^T(\boldsymbol{q}_n) \cdot \left[D_2 L_d(\boldsymbol{q}_{n-1}, \boldsymbol{q}_n) + D_1 L_d(\boldsymbol{q}_n, \boldsymbol{q}_{n+1}) + \boldsymbol{f}_{n-1}^+ + \boldsymbol{f}_n^- \right] = \boldsymbol{0}$$

boundary conditions

$$\boldsymbol{h}_{1d}(\boldsymbol{q}_0, \boldsymbol{p}_0) = \boldsymbol{0} \qquad h_{4d}(\boldsymbol{q}_N) < 0$$

path constraints for $n = 2, \ldots, N$

$$h_{2d}(\boldsymbol{q}_n) = 0 \qquad h_{3d}(\boldsymbol{q}_n) < 0$$

path constraints

for $n = 1, \ldots, \kappa - 2$	for $n = \kappa - 1$	for $n = \kappa + 1, \ldots, N$
$\lambda_{S_n}^3 < 0$	$\lambda_{S_{\kappa-1}}^3 = 0$	$g_S(\boldsymbol{q}_n) > 0$
$\sigma_{LB} < \sigma_1 < \sigma_{OB}$		$\sigma_{LB} < \sigma_2 < \sigma_{OB}$

The final inequalities prevent the time steps 1t and 2t from becoming too little or too big, respectively, during the contact and flight phases, respectively. Furthermore, this provides a minimum and maximum estimate for the overall duration of the manoeuvre.

Conclusion

In this study, we look at a variational integrator that maintains its original structure. Using the straightforward scenario of a one-legged runner as an example, we examine the idea of completely elastic, and therefore fully plastic, contact formulations. Forward dynamics simulations account for contact formulations, with the method calculating contact duration, contact configuration, and force for completely elastic contacts. A perfectly plastic contact model would have the foot remaining planted until the contact force reversed its algebraic sign. In this case as well, the algorithm decides when and how to release the contacts. Additionally, the optimum control issue of a monopodial high leap with a variable time step is solved using a direct transcription approach that makes use of the variational integrator and formulations of the completely plastic contact. Since the contact and flight phases may both be optimized with two scaling factors, the leaping motion is not unnecessarily constrained.

REFERENCES

[1] Aoustin Y., Formalskii A.: Upward Jump of a Biped. Proceedings of the Multibody Dynamics 2011, ECCOMAS Thematic Conference, 4-7 July 2011, USB, Brussels, Belgium.

[2] Betsch P., Steinmann P.: Constrained integration of rigid body dynamics. Comput. Methods Appl. Mech. Engrg., 2001, Vol. 191, pp. 467-488.

[3] Bertsch P.: The discrete null space method for the energy consistent integration of constrained mechanical systems Part I: Holonomic constraints. Computer Methods in Applied Mechanics and Engineering, 2005, Vol. 194, pp. 5159-5190.

[4] Betsch P., Leyendecker S.: The discrete null space method for the energy consistent integration of constrained mechanical systems. Part II: Multibody dynamics. Int. J. Numer. Meth. Engrg, 2006, Vol. 67, pp. 499-552.

[5] Djoudi D., Chevallereau C., Aoustin Y.: Optimal reference motions for walking of a biped robot. Robotics and Automation, Proceedings of the 2005 IEEE International Conference, pp. 2002-2007.

[6] Fetacau R.C., Marsden J.E., Ortiz M., West M.: Nonsmooth Lagrangian Mechanics and Variational Collision Integrators. Siam J. Applied Dynamical Systems, 2003, Vol. 2, No. 3, pp. 381-416.

[7] Franc¸ois C., Samson C.: Energy Efficient Control of Running Legged Robots. A Case Study: The Planar One-Legged Hopper. Simulation et optimisation de systemes complexes, Project ` ICARE, 1996, No. 3027.

[8] Gross D., Hauger W., Schnell W., Schroder J.: Technische Mechanik. Band 3: Kinetik. ¨ Springer, Berlin, Heidelberg, 2004.

[9] Kassat G.: Biomechanik fur Nicht-Biomechanker. Fitness-Contur-Verlag, R ¨ odinghausen, ¨ 1993.

[10] Kraft D.: On converting optimal control problems into nonlinear programming problems. Computational Mathematical Programming, 1985, Vol. F15, pp. 261-280.

[11] Koch M.W., Leyen decker S.: Structure preserving simulation of compass gait and monohedral jumping. Proceedings of the Multibody Dynamics 2011, ECCOMAS Thematic Conference, 4-7 July 2011, USB, Brussels, Belgium.

[12] Koditschek D E., Buehler M.: Analysis of a Simplified Hopping Robot. International Journal of Robotics Research, 1991, Vol. 10, pp. 587-605.

[13] Leyendecker S., Marsden J.E., Ortiz M.: Variational integrators for constrained dynamical systems. ZAMM, 2008, Vol. 88, No. 9, pp. 677-708.

[14] Leyendecker S., Ober-Blobaum S., Marsden J.E., Ortiz M.: Discrete mechanics and optimal ¨ control for constrained systems. Optimal Control Applications & Methods, 2009, Vol. 31, pp. 505-528.

[15] Leyendecker S., Hartmann C., Koch M.W.: Variational collision integrator for chains. J. Comput. Phys., 2012, DOI 10.1016/j.jcp.2012.01.017, Vol. 231, p. 3896-3911.

[16] Marsden J.E., West M.: Discrete mechanics and variational integrators. Acta Numerica, 2001, Vol. 10, pp. 357-514.